SCALING OF LOCAL TRANSPORT IN JET ELMY H-MODE DISCHARGES WITH H, D, DT, AND T ISOTOPES

R.V. Budny[1], B. Balet, D. Bartlett, J. Christiansen, J.G. Cordey, D.R. Ernst[1], G. Fishpool, C. Gowers, L. Horton, A.C. Howman, J. Jacquinot, C. Lowry, K. Thomsen, B. Tubbing, B. Schunke and D. Start

JET Joint Undertaking, Abingdon, OX14 3EA, UK
[1]*Princeton University, PPPL, P.O.Box 451, Princeton NJ 08543, USA*

1. Introduction

The thermal energy confinement time in JET H-mode plasmas has a weak scaling with the isotopic mass A [1] whereas in TFTR supershots and L-mode plasmas, it has a stronger scaling [2,3]. We use the TRANSP plasma analysis code[4,5] to study transport in ELMy H-mode plasmas to gain a deeper insight into the A dependence.

2. Data and Analysis

Experiments were performed in JET to study the scaling of ELMy H-mode discharges with dimensionless parameters such as the gyro-radius normalized by the minor radius $\rho_* \equiv \rho / a$, collisionality ν_*, normalized thermal pressure β, Mach number of the toroidal rotation M_a, and the isotopic mass of the thermal hydrogenic species A, defined by

$$A \equiv < n_H + 2n_D + 3n_T > / < n_H + n_D + n_T > \qquad (1)$$

Several methods were used to vary these parameters. For instance, the plasma current I, and toroidal field B, which were maintained in a constant ratio, were varied from discharge to discharge. Typical values scanned were I[MA] ≈ B[T] ≈ 1, 1.8, 2, 3, and 3.8. The mass A was varied by changing the neutral beam injection (NBI) species and target plasma species from H to D to T. The total neutral beam heating power was varied up to 22MW. The discharges achieved quasi-steady state conditions during the ELMy phase. The ratio T_e / T_{ion} was approximately 1 in the core.

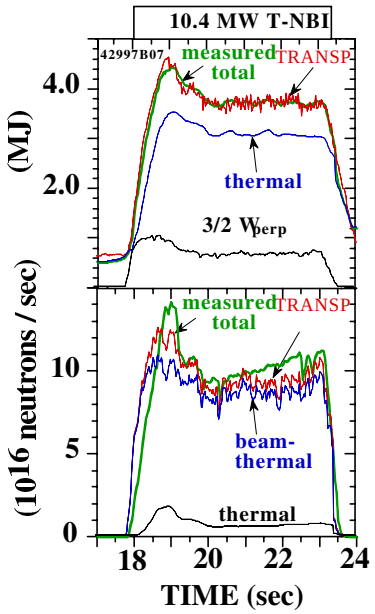

Fig. 1. Comparison of measured and calculated global parameters. The database time is 20.6 s.

TRANSP uses measurements such as profiles for n_e, T_e, T_{ion}, Z_{eff}, and the toroidal rotation of the C impurity. Since ECE measurements of T_e are not available throughout the wide range of B considered, we use the T_e measured by LIDR. Examples of checks on the accuracy of the modeling are shown in **Fig. 1**. More than 50 of these H-mode discharges are analyzed. A database was constructed from the results at a representative time

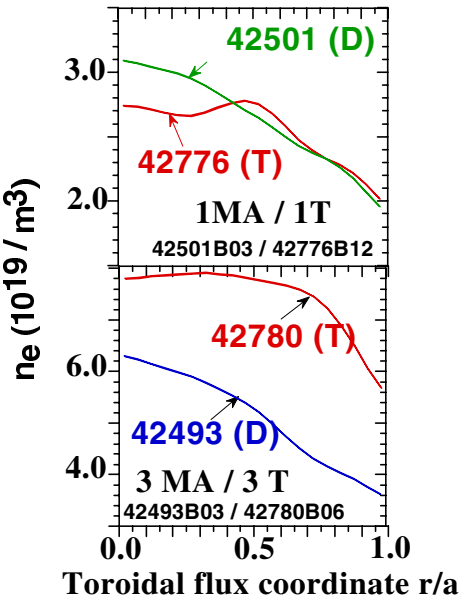

Fig. 2. Comparison of n_e profiles for D-only and T-only pairs with similar P_{NBI}

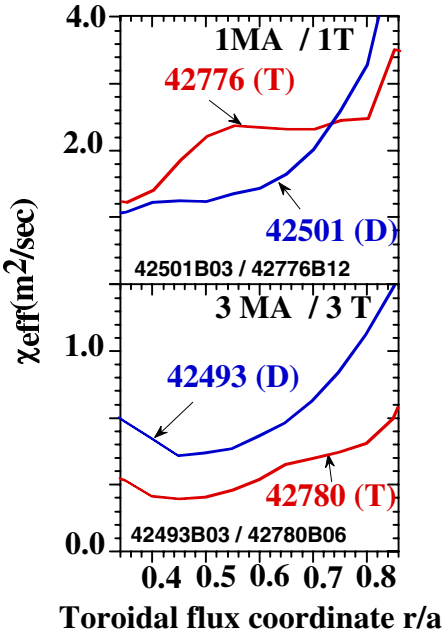

Fig. 3. Comparison of χ_{eff} profile for the pairs in Fig. 2.

during their ELMy phases. The computed A profiles are approximately constant in radius during the selected times, ranging in values from approximately 1 to 3. Values of the normalized thermal β_n ranged from 0.5 to 3.5, and M_a in the center ranged from 0.05 to 0.8.

We studied systematic trends in plasma parameters with A. The ratio of the computed and measured stored energy is ≈ 1.1±0.1, with a slight trend to increase with A. The n_e values tend to increase with A, especially at higher values of I ≈ B. Examples of the profiles for two pairs are shown in **Fig. 2**. The peaking of the n_e profiles tends to decrease systematically to 1 at A=3. Since the fueling rate from T-NBI is less than that of D- and H-NBI at the same power and voltage, n_e might be expected to have the opposite trend. The observed trend is confirmed by the calculated effective particle diffusivity D_e, which decreases with A. Examples of the profiles for the effective energy transport coefficient χ_{eff} are shown in **Fig. 3**.

3. Results at the half-radius

This paper focuses on results at the half-radius since this region is sufficiently far from the center to minimize sawtooth effects, and sufficiently far from the separatrix to minimize ELM-induced oscillations. The negative inverse scale-length of n_e, $-L_{ne}^{-1} \equiv -(\nabla n_e) / n_e$, decreases towards zero with A. This is shown in **Fig. 4-a**. The inverse scale-lengths of the ion and electron temperatures show less variation with A. Their magnitudes are $-L_{Ti}^{-1} \approx 1.7\pm0.4$ /m, and $-L_{Te}^{-1} \approx 1.4\pm0.6$ /m. The ratio of the temperatures, T_{ion} / T_e is ≈ 0.85±0.15. The ratio of D_e and χ_{eff} decrease with A, as shown in **Fig. 4-b**. The values of M_a at the half-radius are relatively high, as shown in **Fig. 4-c**, especially for the D-only-NBI pulses. Although the T-NBI injects more torque per beam ion, the deposition tends to be further from the center.

Regression analysis is used to study the scaling of the TRANSP-determined thermal energy confinement time at the half radius, τ_{th}. Regression using the engineering parameters B, volume-averaged $n_e[10^{19}\ /m^3]$, loss power P_{loss} [MW], and A gives

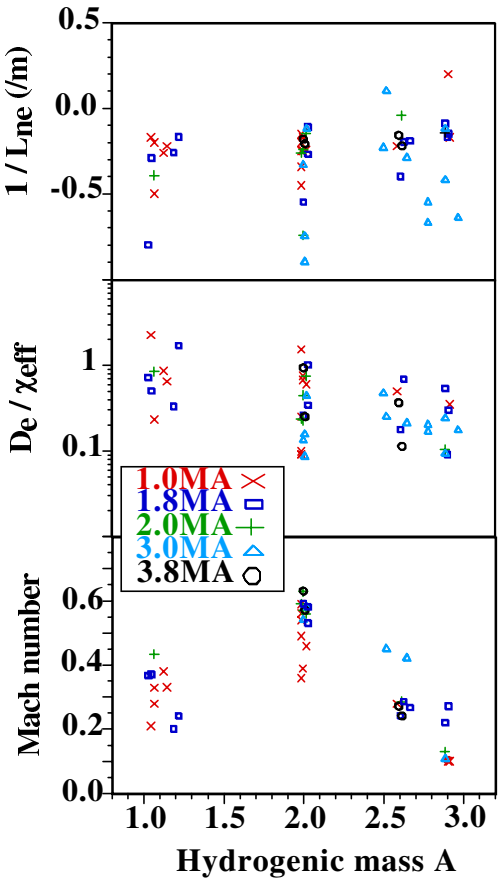

Fig. 4. Trends of plasma parameters at the half radius versus the hydrogenic mass A

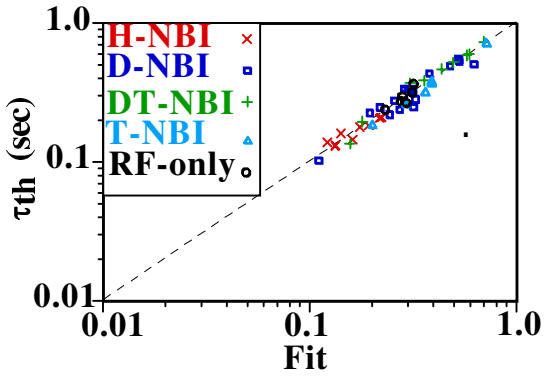

Fig. 5. TRANSP-calculated thermal energy confinement time and the fit in Eq. 2-a.

$$\tau_{th}\,[\mathrm{sec}] \approx 0.144\, B^{a}\, n_e^{\,b}\, P_{loss}^{\,c}\, A^{d} \qquad (2\text{-a})$$

with a ≈ +0.64±0.05, b ≈ +0.68±0.05, c ≈ -0.60±0.04, and d ≈ +0.26±0.05. The R^2 for this fit is 96%. This is shown in **Fig. 5**. The ratio of the TRANSP τ_{th} and this fit does not show systematic variations with parameters such as the ELM frequency, M_a, L_{ne}, or L_{Te}. It does have a tendency to decrease with increasing $-L_{Ti}^{-1}$. The ratio of the TRANSP-determined τ_{th} at the full- and half-radii is ≈ 1.3±0.4. Regression gives a fit for τ_{th} at the full radius with powers very similar to those in Eq.(2-a).

A pedestal in the T_e profile is measured with ECE. Assuming $T_e = T_{ion}$ at the top of the pedestal, the pedestal energy W_{ped} was computed for half the discharges in the database. Subtracting W_{ped} from the thermal energy at the full radius gives a corrected "core" energy. Using P_{loss}, a "core" energy confinement time at the full radius, τ_{core} can be derived [6]. The fit for τ_{core} using the TRANSP results has a weaker A scaling than Eq. (2-a), $\propto A^{d}$ with d ≈ +0.09±0.11.

We use dimensional scaling with the constraints for the collisional high β regime to translate the fit in Eq. (2-a) to one using the dimensionless parameters ρ_*, ν_*, β, and A. The result is

$$(B / A)\,\tau_{th} \propto \rho_*^{\,a}\, \nu_*^{\,b}\, \beta^{c}\, A^{d} \qquad (2\text{-b})$$

with a ≈ -2.71, b ≈ +0.16, c ≈ -0.08, and d ≈ +1.06. This has a gyro-Bohm-like dependence, and is very similar to the ITERH-EPS97(y) scaling [1]. However the β dependence is much weaker. Direct regression using the database values gives a fit similar to Eq.(2-b). The same dimensional scaling arguments for τ_{core} imply $\tau_{core} \propto A^{d}$, with d ≈ +0.5; however there is considerable uncertainty in the exponent.

Turning to the scaling of χ_{eff}, the examples in Fig. 3 suggest that at low I ≈ B, χ_{eff} in T is higher than in D, whilst at the higher I ≈ B the relation is reversed. A simple regression for χ_{eff} using dimensionless variables gives the fit,

$$(A / B / a^2)\, \chi_{eff} \approx 82\, \rho_*^{\,a}\, \nu_*^{\,b}\, \beta^c\, A^d \qquad (3)$$

with a ≈ +2.9±0.2, b ≈ +0.21±0.09, c ≈ -0.56±0.2, and d ≈ -0.46±0.13. The R^2 for this fit is 86%. The relatively large scatter in the fit suggests that the dependencies such as L_n or M_a may be important in view of the contradictory A dependence of the 1MA and 3MA discharges, shown in **Fig. 3**.

We expect different scaling for the electron and ion thermal heat transport coefficients, χ_e and χ_{ion}, and for the toroidal angular momentum transport χ_ϕ, and for D_e. For instance, the Ion Temperature Gradient (ITG) modes are expected to affect χ_{ion} more directly, while the trapped electron response can contribute significantly to χ_e or D_e with different A dependencies [7,8]. The computed ratio of χ_{ion} and χ_{eff} is approximately 1.5±0.7. The computed ratio of χ_ϕ and χ_{eff} is approximately 0.7±0.4. These do not exhibit significant variation with A. The values for χ_e at the half-radius are computed with less accuracy. The ratio of χ_e and χ_{eff} tends to increase with A.

4. Discussion

The scaling of τ_{th} is found to be weakly dependent on the effective mass A, especially at low I ≈ B, in contrast with supershots in TFTR. In terms of the dimensionless parameters ρ_*, ν_*, and β, τ_{th} is found to scale in a Gyro-Bohm like fashion similar to the global confinement expression for ELMy H-mode ITERH-EPS97(y). However the β dependence is much weaker than EPS97(y) and in accord with the transport being small scale (ρ_{ion}) electrostatic turbulence. χ_{eff} is found to increase with mass A at low I ≈ B where the density profiles are well matched, but it decreases at higher I ≈ B where the density profiles are not matched. Further work is required to establish the dependence of χ_{eff} on the unmatched dependencies such as L_{Ti}, L_n, and the rotation Mach number.

Acknowledgements

Work supported in part by US DoE Contract No. DE-AC02-76-CH03073.

References

[1] J.G. Cordey, et al.: Plasma Phys. & Cont. Fusion **38**, 115 (EPS, 1997).
[2] R.V. Budny, M.G. Bell, et al.: *Proceedings 1994 EPS Conference*, **I**, 82.
[3] S.D. Scott, G.W. Hammett, et al.: *IAEA Fusion Energy Conference* (Montreal, 1996).
[4] R.V. Budny, M. G. Bell, H. Biglari, et al.: Nucl. Fusion **32**, 429 (1992).
[5] B. Balet, P.M. Stubberfield, D. Borba, et al.: Nucl. Fusion **33**, 1345 (1993).
[6] K. Thomsen, et al.: *invited paper, this conference* (1998).
[7] F.Y. Gang, P.H. Diamond, and M.N. Rosenbluth: Phys. Fluids **B3**, 68 (1991).
[8] T.S. Hahm: Phys. of Fluids, **B3**, 1445 (1991).